Int J Adv Manuf Technol (2011) 57:617–637
DOI 10.1007/s00170-011-3302-x

ORIGINAL ARTICLE

An experimental investigation into the micro-electrodischarge machining behavior of p-type silicon

Muhammad Pervej Jahan · T. W. Lieh · Yoke San Wong · Mustafizur Rahman

Received: 6 September 2010 / Accepted: 24 March 2011 / Published online: 4 May 2011

Abstract The present study aims to investigate the feasibility of micro-structuring in p-type silicon, using conventional die-sinking electrodischarge machining (EDM). The EDM behavior of the silicon material is studied in terms of the effect of major operating parameters on the performance characteristics during the micro-hole machining. In addition, microelectrodes are fabricated successfully on the conventional EDM machine for machining different micro-structures in silicon. Three different types of micro-structures—micro-hole, blind slots, and through slots—are fabricated in p-type silicon successfully by using optimum parameters setting. It has been observed that p-type silicon is machinable by EDM using both the polarities. Moreover, like other electrodischarge machinable materials, the selection of optimum operating parameters is very important for improved performance, as those parameters are found to influence the EDM performance of silicon significantly. Finally, it has been concluded that p-type silicon is machinable into different forms of micro-structures by understanding its electrodischarge machining behavior and by careful selection of optimum parameters.

Keywords p-type silicon · Micro-EDM · Micro-hole · Micro-slots

Electronic supplementary material The online version of this article (doi:10.1007/s00170-011-3302-x) contains supplementary material, which is available to authorized users.

M. P. Jahan (✉)
Department of Mechanical Engineering, University of Arkansas, Fayetteville, AR, USA
e-mail: mjahan@uark.edu

T. W. Lieh · Y. S. Wong · M. Rahman
Department of Mechanical Engineering, National University of Singapore, Singapore 119260, Singapore

1 Introduction

As the world moves into the twenty-first century, the technology is moving toward the production of miniaturized and even microscopic components. As devices shrink in size, the components that make up these devices have to be shrunk even further and thus the need for micro-machining to produce these devices. The need for smaller silicon chips with greater capabilities is ever increasing with the rise of personal computers, laptops, palmtops, and even mobile phones, as those products are fighting to decrease in size and more commonly they all have silicon memory chips in them.

Presently, the production of silicon chips is mainly by etching, deposition, and other photolithographic techniques [1]. The limitation of these techniques is that they are only two-dimensional, with the exception of etching which can be done selectively and in layers to attain three-dimensional features. Machining of silicon using tools can only be done using the EDM or micro-EDM for smaller parts [1]. This is so because in EDM, there is no actual contact between the tool and the workpiece. This makes EDM suitable for the machining of silicon, which is brittle by nature as the large cutting force of the other tooling methods will break the workpiece during machining. EDM or spark machining removes electrically conductive material by means of rapid, repetitive spark discharges from electric pulse generators with the dielectric flowing between the tool and the workpiece. EDM has the advantages of producing three-dimensional and complex profiles in the workpiece. The electrodes are cheap and easier to manufacture as compared with the cutters of the other tooling methods or the masks used in etching. EDM is very flexible thus making it ideal for prototypes or small batches of products with a high added value.

Micro-electrodischarge machining of silicon is a relatively new area with potential in the silicon industry. With the increasing interest in micro-electromechanical systems (MEMS), the researchers were re-investigating all traditional manufacturing techniques in order to produce micro-mechanical parts and EDM was found to be highly suitable. Some of the first to report experiments with EDM of silicon was Masaki and his team [2]. They machined 330-μm-thick silicon wafers with resistivity between 10 and 100 Ω cm. They found out that the machining speed of silicon is almost double that of stainless steel, while the frontal electrode wear was lower. Another group of researchers, Lou and his team [3, 4], used wire EDM to cut n-type single-crystal silicon ingots with the resistivity of 7–15 Ω cm. The wire was made of molybdenum, with a diameter from 50 to 140 μm. The dielectric used was kerosene. They succeeded in slicing wafers of 94 to 210 μm thickness using an n-type silicon ingot with resistivity of 7–15 Ω cm and plated with nickel to reduce surface contacts. The machining speed was 170 mm^2/min. They also reported that the roughness increases when higher machining speeds are used. Moreover, using EDM, Langen and his team [5] developed a system for modular machining and assembly of three-dimensional micro-parts with self-alignment. In this system, the micro-parts and their micro-tools are machined by EDM and temporarily stored in a mini-worktable of a modular machining assembly (MMA). In this MMA, further machining and assembling has been performed, and a self-aligned pin-plate module has been fabricated. In addition, a planner silicon spring has been fabricated laterally out of a (100)-oriented silicon wafer using wire EDM by Staufert and his team [6]. A thermal annealing step and an isotropic etching process were used to restore the crystalline structure of the silicon wafer. The spring was exposed to three million cycles without detecting any fatigue. This spring was used for multi-position measurement of mechanical parts.

Another group of researchers—Reynaerts et al.—have studied micro-EDM of n-type silicon in great details in the past few years [1, 7, 8]. They were able to manufacture a cylindrical electrode of diameter 34 μm and length 1,170 μm using a sacrificial workpiece. The electrode has cylindricity better than 1 μm and its roughness better than 2 μm. With a slight modification to their previous method, they were able to reduce the electrode diameter down to 12 μm over a length of 250 μm keeping the roughness better than 2 μm and cylindricity better than 1 μm. Having mastered on the machining of axisymmetric electrode, they proceeded to machine electrodes of polygonal cross sections. A triangular electrode of 37 μm on each side 772 μm long and a rectangular electrode of 19×26 μm with length 758 μm had been produced. Using a combination of machining techniques including EDM, they were able to machine the rotor of an elastic force motor, to produce 45° mirrors for optical fibers, acceleration sensors, and micro-springs. Reynaerts and his team also looked into the production of seismic mass suspensions in n-type silicon using EDM [9, 10]. The aim of the research was to produce a resonant beam accelerometer structure which consists of a seismic mass suspended by eight beams: four suspension beams and four resonating beams. The sensing principle is based on a shift in resonance frequency of the resonating beams induced by the acceleration forces. However, the major problem in the design was the machining of such a complex sensor structure in silicon. Originally, a structure of two bonded wafers was proposed, but the problem of alignment cannot be solved. Thus, it was decided to manufacture a monolithic sensor structure using EDM. Moreover, in recent year, investigation has been carried out on the fabrication of high aspect ratio silicon microelectrode arrays by micro-wire electrical discharge machining (μ-WEDM) [11]. Arrays with 144 electrodes on a 400 μm pitch were machined on 6- and 10-mm-thick p-type silicon wafers to a length of 5 and 9 mm, respectively. Most of these researches focused on the micro-structuring of silicon for different applications without providing detail discussion on the electrodischarge machining behavior of silicon.

In addition to research on micro-structuring of silicon, some investigation has been reported on the fundamental studies on the EDM and WEDM of silicon material. An experimental investigation has been carried out to improve the machining rate of EDM for silicon single crystals by reducing the contact resistance between the silicon single crystal and metal electric feeder [12]. In order to decrease the resistance of the rectifying contact between a p-type silicon wafer and the metal feeder, attempts have been taken to achieve ohmic contact by plating the contact surface of the silicon wafer with aluminum by vacuum evaporation, followed by the diffusion process. Furthermore, a series of experiments has been carried out to machine smoothly polished single-crystal p-type silicon plates by WEDM in water and oil, in order to investigate the effect of WEDM on the polished surfaces [13]. The experimental findings suggest that there is a formation of silicon oxide due to electrodischarge machining, which makes the surface rougher. However, for cutting in oil, polished surfaces near a cut section are smooth and almost flat although they have chips and cracks. The machining possibilities of silicon wafers by the EDM process are also reported [14]. A fine tungsten carbide rod was machined as tool electrode for EDM process, and micro-components in silicon wafer were processed by EDM process. In addition, several testing experiments were carried out with different process parameters to investigate the influence of the micro-EDM process on the silicon structure [15]. However, in their study, the authors put emphasis on the surface

roughness and on avoiding micro-cracks generated by the sparking process. They showed that micro-structures with a sufficiently low surface roughness and with small micro-cracks can be produced. Although several studies have been carried out on the EDM and micro-EDM of silicon, a number of important issues like understanding the process mechanism, machining behavior of silicon, selection of optimum parameters for micro-structuring in silicon, etc. remain to be unsolved before electrodischarge machining becomes a reliable process for micro-manufacturing of silicon-based products for semiconductor industries and MEMS.

Although several micromachining processes can be used for machining silicon, micro-EDM has clearly some advantages over the other existing processes. While micro-grinding process is already an established process for machining silicon, the majority of the applications are limited to surface application only. It is very difficult to apply micro-grinding process for micro-structuring in silicon. The force generated from the micro-grinding process makes it difficult to apply for micro-structuring in silicon. The laser micromachining may be a suitable alternate of micro-EDM for the micro-structuring of silicon. However, the surface obtained in laser machining is more susceptible to materials damage such as melting, thermal degradation, heat affected zones, craters, and cracks compared with that obtained using EDM. Therefore, investigating the feasibility of machining silicon using micro-EDM and understanding the micro-electrodischarge machining behavior of silicon is of prime importance.

In this study, the authors will attempt to look into the various aspects of machining during the micro-EDM of silicon workpiece. The relations between operating parameters and performance characteristics were studied for a wide range of values for each parameter, which will help in better understanding, control, and predictable selection of operating parameters for micro-structuring in silicon. Finally, three different types of micro-structures—micro-hole, blind slots, and through slots—were machined successfully by using optimum parameters setting in electrodischarge machining of p-type silicon.

2 Experimental setup and procedure

2.1 Machine tool

The machine used for this experiment is the Roboform 40 produced by Charmilles Technologies [16]. It is energized by a 64-A transistor type pulse generator. The machine is made of four main elements, namely the central control unit, the work tank, the position control, and the dielectric tank. The *central control unit* manages the operation between the operator and the machine and also those between the different elements of the machine. It also houses the memory units and the power supply. The servo control unit monitors and determines the advancement of the electrode toward the workpiece. The servo is expressed in percentage and varied from 0% to 100%. The *work tank* is where the workpiece will be clamped, and it is designed to machine when the workpiece is covered with a minimum 40 mm of dielectric to prevent fire risks. Two sides are in the form of a double-hinged door for easy access to the workpiece. It can take a maximum workpiece weight of 1,000 kg. The *position control* determines the motion of the tool electrode in the *X*-, *Y*-, *Z*-, and *C*-axis, the movement is controlled by servo motors, and it also controls the speed of descend of electrode onto the workpiece as determined by the servo parameter. The position accuracy and resolution in all three axes are 0.00002 in. The *dielectric tank* stores the dielectric and has a capacity of 500 l. It consists of an electrovalve for filling and emptying and pumps to fill and maintain the dielectric level in the work tank. The *rotating unit* 3R-1.321 HS is added to provide rotation of the electrode. It is a belt-driven mini-chuck holder with rotation speed up to 2,000 rpm. Figure 1 shows schematic diagram of the basic units of the EDM system.

2.2 Materials

The material selected for the tool electrode is tungsten, and the specifications are shown in Table 1. The tungsten electrode has been used for its high melting point and high wear resistance. The workpiece is p-type silicon, and the specifications are shown in Table 1. The dielectric used is hydrocarbon oil EDM 22 having relatively high flash point, high auto-ignition temperature, and high dielectric strength. It is also chosen for its low volatility and low aromatic content. The specifications are presented in Table 2.

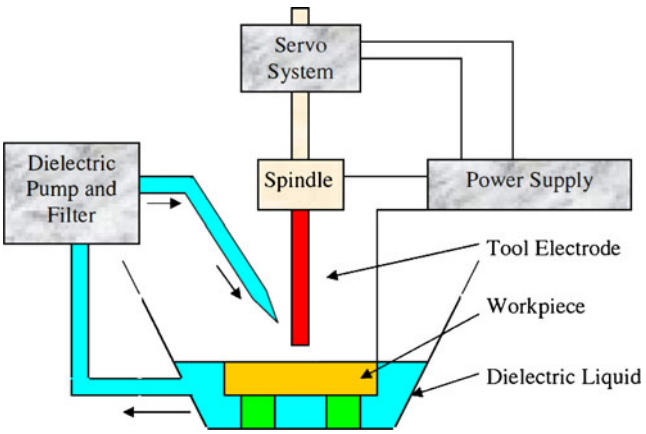

Fig. 1 Schematic diagram showing the basic elements of the EDM system

Table 1 Properties of tungsten electrode and silicon workpiece [17]

Material	Tungsten	Silicon
Atomic number	74	14
Crystal structure	Body-centered cubic	Tetrahedral cubic amorphous
Density, kg/m^3	19,300	2,490
Melting point, °C	3,370	1,414
Boiling point, °C	5,930	2,600
Electrical resistivity (at 23°C), Ω cm	5.65×10^{-6}	0.002
Young's modulus, N/m^2	345×10^9	112.4×10^9
Hardness	255 DPN	–

2.3 Experimental procedure

The experiments were conducted in three parts. The first part is to machine micro-holes using 200-μm-diameter electrodes in a p-type silicon workpiece of 0.5 mm thickness. The effect of operating parameters on the performance parameters for the process was also studied. In the second part, the microelectrodes were fabricated on-machine from 0.5 mm diameter to about 40–50 μm in diameters, and these microelectrodes are then used to machine the silicon workpiece of same 0.5 mm thickness with focus in investigating feasibility of achieving smaller and high aspect ratio micro-holes. Finally, machining of both blind and through slots was also attempted in this study. The slots are machined to a depth of 0.3 mm for the blind slots while the through slot is machined to a depth of 0.8 mm. The electrodischarge machining behavior of the p-type silicon workpiece is investigated based on micro-hole machining, blind slot machining, and through slot machining. The performance parameters are calculated and studied for each process. Equations 1, 2, and 3 present the calculation of material removal rate (MRR), wear ratio (WR) and taper from the micro-hole and tool geometry as shown in Fig. 2. A brief explanation of the performance parameters are presented below, which will help in understanding the effect of operating parameters on the performance characteristics during EDM of p-type silicon.

Material removal rate The MRR determines the speed at which machining takes place and calculated as the total volume of material removed per unit time. MRR can be calculated from the weight difference of the material before and after machining and also from the geometry. For micro-hole machining as the MRR is very small, therefore the difference in weight will be also very small, which may lead to an error if calculated by weight difference method. In this study, it can be obtained using the following equation from the geometry of the micro-hole [18]:

$$\mathrm{MRR} = \{\frac{\pi}{4}[\frac{(D_t + D_b)}{2}]^2 \times L\} \div t \quad (1)$$

where t is the machining time, D_t and D_b are the top diameter and bottom diameter of the micro-hole respectively, and L is the workpiece thickness.

Electrode wear ratio There are many ways that the electrode can be worn off. These include the corner wear, frontal, and lateral wear. For this study, the author will only investigate the frontal electrode wear that is the difference in length of the electrode before and after machining. Therefore, any reference to electrode wear in this report will mean frontal electrode wear. The wear ratio is ratio of volume of tool material worn off to the volume of workpiece material removed. Large values will mean that the tool will have to be changed more regularly and too

Table 2 Specifications of EDM 22 dielectric oil

EDM	Units	Methods	Values
Appearance	–	Visual	Transparent
Density	kg/m^3	ISO 3675	812
Color	–	ASTM D158	0.5
Viscosity at 20°	mm^2/s	ISO 3104	34
Flash Point Pensky-Martens	°C	ISO 2719	102
Pour point	°C	ISO 3016	−50
Total aromatic content	wt.%	TOTAL IL 14 (DMSO-UV)	0.01
Distillation range	°C	ISO 3405	230/270

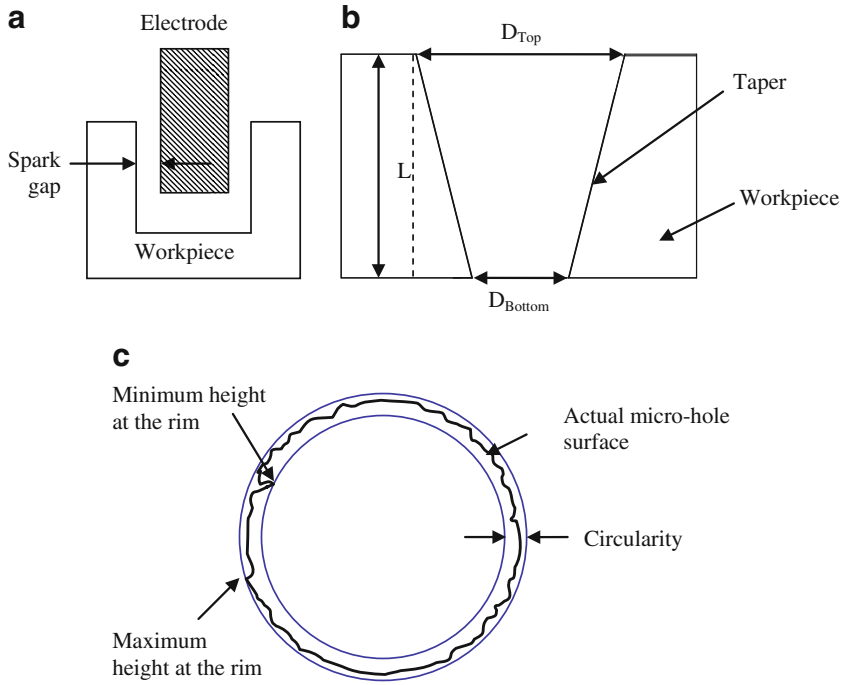

Fig. 2 Schematic presentation of measurement of **a** spark gap, **b** taper, and **c** circularity from the micro-hole geometry

wear can also affect the workpiece finished profile. WR can be calculated using the following equation:

$$\mathrm{WR} = \frac{\mathrm{TWR}}{\mathrm{MRR}} \tag{2}$$

where TWR (frontal) is the volumetric frontal tool wear rate given by $\mathrm{TWR} = \frac{\pi D^2 T}{4t}$, T is the frontal electrode wear, and D is the tool diameter.

Taper Due to lateral electrode wear, the diameter of the hole on the top surface will be slightly larger than that on the bottom surface as shown in Fig. 2b. This value can be obtained by the following equation:

$$\mathrm{taper} = \frac{D_\mathrm{t} - D_\mathrm{b}}{2L} \tag{3}$$

where D_t and D_b are the top diameter and bottom diameter, respectively, and L is the depth of hole which is also the thickness of the workpiece for a through hole. Equation 3 represents the tangent value of taper angle ($\tan\theta$) of the micro-hole wall and will be expressed as taper in this manuscript.

Circularity The circularity is the roundness of the machined hole; it is measured using the Kmess softwear of the optical multi-sensor. The values measured is in terms of actual deviation (mm D_A), which is the summation of errors from a perfect circle of the same diameter to the machined circle. First of all, the hole is fitted between the two circles. The outline of the hole is being plotted with 100 points by scanning from inside to outside of the rim (Fig. 2c). From the plotted points, the maximum peak-to-valley values of the machined surface is then measured and reflected as the circularity of the hole.

2.4 Experimental measurement and analysis

For measuring dimensions of the micro-holes and micro-slots, the Keyence VHX Digital Microscope (VH-Z450) was used. A Mahr Optical Multi-sensor was used for measuring the circularity of the machined micro-holes. "Kmess" software associated with the optical multi-sensor is used for measurement of circularity.

3 Results and discussion

3.1 Effect of gap voltage

The effect of gap voltage on the performance of micro-EDM of p-type silicon is shown in the Fig. 3. The other parameters are kept unchanged. The parameter settings are peak current of 3 A, pulse duration (T_on) of 25 μs, pulse interval (T_off) of 50 μs, servo of 65%, and electrode rotational speed of 1,200 rpm.

The gap voltages are varied for six different settings: 120, 160, 200, −120, −160, and −200 V for studying the effect of gap voltage on different performance parameters. It has been observed that the MRR is higher for larger gap voltage and decreases as the voltage decreases. The relationship is approximately linear for both the positive and the negative values of

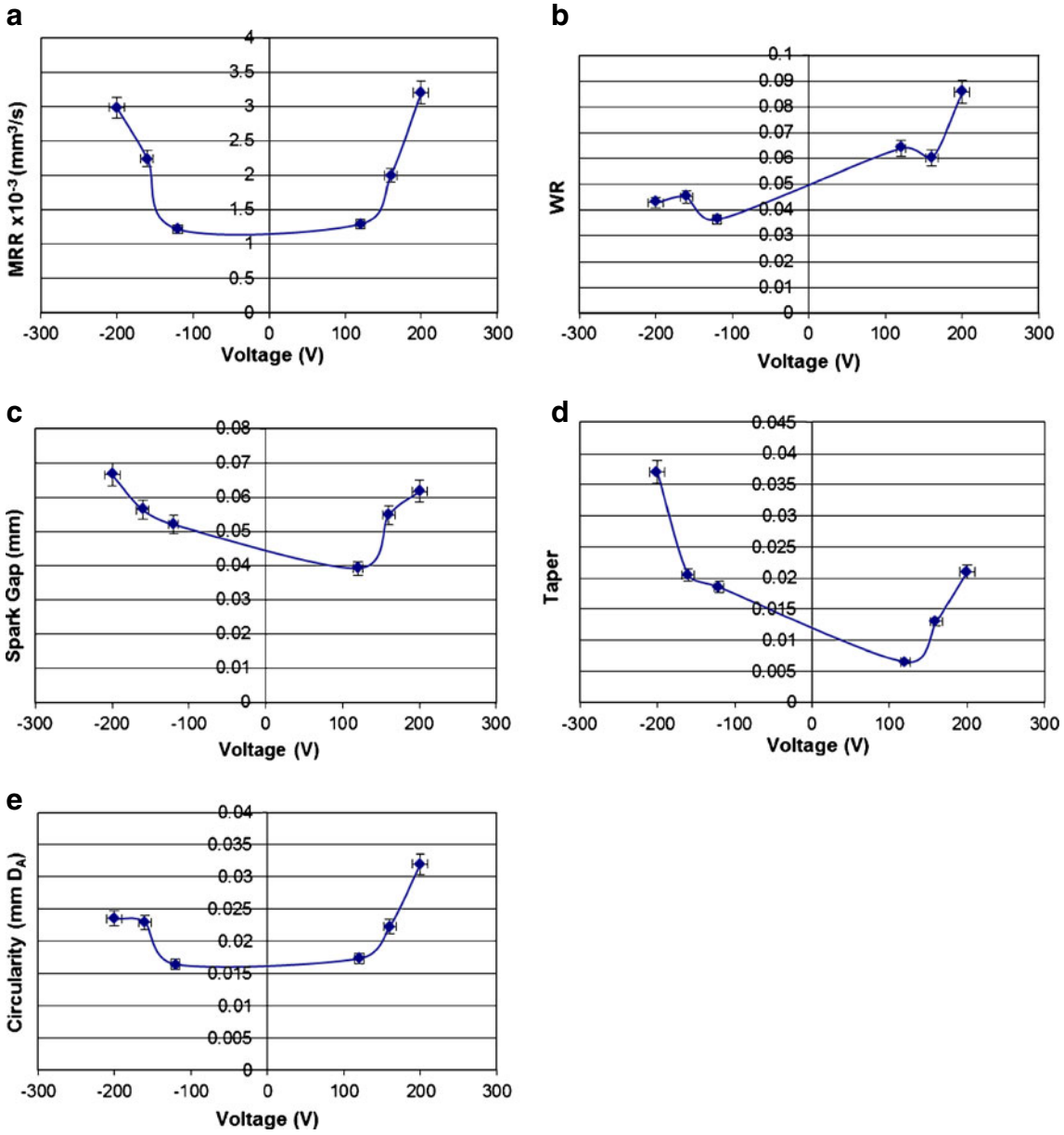

Fig. 3 Effect of voltage on **a** MRR, **b** WR, **c** spark gap, **d** taper, and **e** circularity of the micro-holes

the gap voltage. However, the MRR is slightly higher for positive voltages, and this tendency is due to alignment of the p-type silicon favoring positive voltages. The spark gap is also bigger for larger values of voltage and positive voltage produce holes with smaller spark gaps. The smallest spark gap is obtained when 120 V is used, and the value is 0.0392 mm. Therefore, it has been observed from Fig. 3 that with the increase of gap voltage, the gap width increases as the higher voltage allows breakdown of dielectric at a wider gap due to the higher electric field. However, the taper is the smallest when the voltage is 120 V. This could be due to the fact that the lateral tool wear becomes more prominent as the electrode size gets smaller in higher voltage. Therefore, the smaller voltage has a smaller taper in the case of the 0.2-mm electrode.

For positive voltages, the WR is the lowest at 160 V and the highest at 200 V. For negative values of voltage, it is reversed, with −160 being the highest and −120 being the lowest (see Figs. 4 and 5). However, the WR for positive voltages are very much higher than those of negative values of voltage. It is noted thus that positive values of voltage not only give high MRR but tool wear is also large. If tool wear is of concern to machining, negative values of voltage should be used. The holes produced by using high voltages are not as round as those produced using smaller voltages regardless of polarity. Positive voltages produce holes that are generally less round, as shown by the large values of

Fig. 4 Comparison of performance parameters at the lowest and highest setting of voltage (at positive polarity)

a

Fixed Parameters	Peak Current	Pulse Duration	Pulse Interval	Servo	Tool Diameter	Rotation
	3 A	25 µs	50 µs	65	200µm	1200 rpm

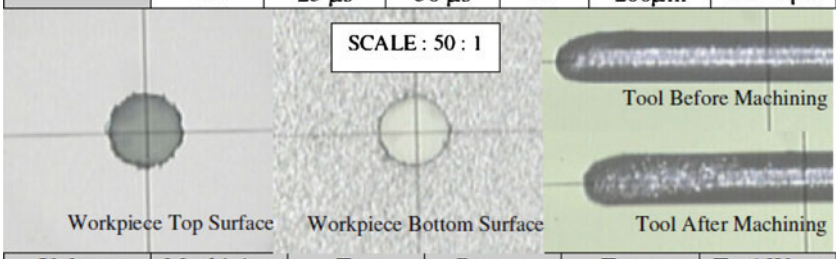

Voltage	Machining Time	Top Diameter	Bottom Diameter	Taper	Tool Wear
120 V	23 s	278.5 µm	272.0 µm	0.0065	60.5 µm

MRR x 10^{-3}	WR	Spark Gap	Circularity
1.2935 mm^3/s	0.0638	0.0392 mm	0.0173

b

Fixed Parameters	Peak Current	Pulse Duration	Pulse Interval	Servo	Tool Diameter	Rotation
	3 A	25 µs	50 µs	65	200µm	1200 rpm

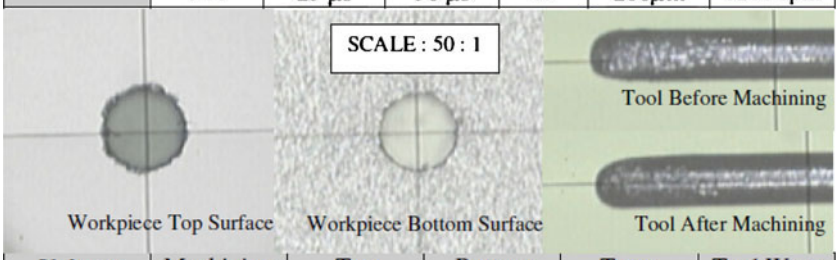

Voltage	Machining Time	Top Diameter	Bottom Diameter	Taper	Tool Wear
200 V	12 s	323.5 µm	302.5 µm	0.0210	105.0 µm

MRR x 10^{-3}	WR	Spark Gap	Circularity
3.2060 mm^3/s	0.0857	0.0617 mm	0.0320

actual deviation, than negative voltages. It can be seen from Figs. 4 and 5 that, for both the cases of 120 and 200 V, the negative polarity provided slightly lower circularity than that of positive voltages, which means the surfaces at the rim of the micro-holes are smoother for negative polarity compared with that of positive polarity.

Comparing the overall performance parameters for positive and negative polarity as shown in Figs. 4 and 5, it has been confirmed that positive polarity exhibits better performance for the micro-EDM of silicon. Although positive polarity provides slightly higher circularity at the rim of micro-holes, it exhibits better performance by providing higher MRR and significantly lower spark gap. The MRR is very important, as the productivity is the main concern during the production of batch mode micro-structures. Moreover, lower spark gap ensures more stable dimensional accuracy of the micro-holes. Therefore, for comparison of performance parameters at the highest and lowest setting of different operating parameters, the experiments are conducted using positive polarity.

3.2 Effect of peak current

The effect of peak current on different performance parameter is shown in Fig. 6. The machining conditions are set at a voltage of 200 V, pulse duration of 25 µs, pulse interval of 50 µs, servo of 65%, and electrode rotational speed of 1,200 rpm.

The MRR decreases until 4 A, where it increases again with further increase of peak current. The decrease could be due to the fact that when using high currents, too much material is melted during each spark and cannot be flushed away in time and re-solidified in the hole. The re-solidified material may be harder to machine therefore increasing the

a

Fixed Parameters	Peak Current	Pulse Duration	Pulse Interval	Servo	Tool Diameter	Rotation
	3 A	25 µs	50 µs	65	200µm	1200 rpm

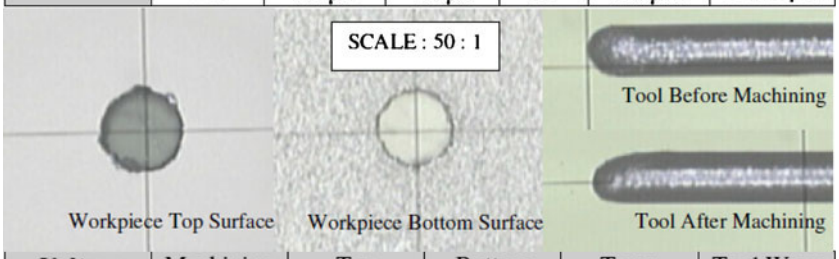

Voltage	Machining Time	Top Diameter	Bottom Diameter	Taper	Tool Wear
-120 V	28 s	304.0 µm	285.5 µm	0.0185	39.5 µm

MRR x 10^{-3}	WR	Spark Gap	Circularity
1.2184 mm^3/s	0.0363	0.0520 mm	0.0164

b

Fixed Parameters	Peak Current	Pulse Duration	Pulse Interval	Servo	Tool Diameter	Rotation
	3 A	25 µs	50 µs	65	200µm	1200 rpm

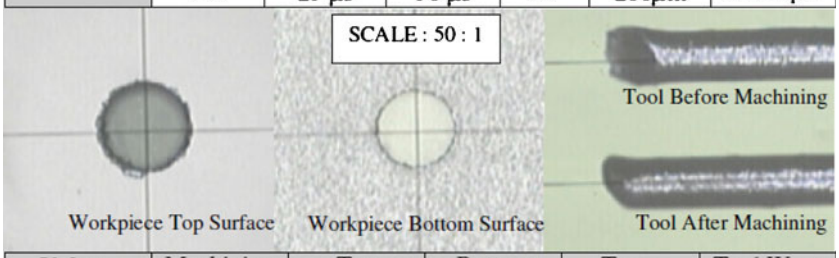

Voltage	Machining Time	Top Diameter	Bottom Diameter	Taper	Tool Wear
-200 V	13 s	333.0 µm	296.0 µm	0.0370	53.0 µm

MRR x 10^{-3}	WR	Spark Gap	Circularity
2.9878 mm^3/s	0.0428	0.0665 mm	0.0235

Fig. 5 Comparison of performance parameters at the lowest and highest setting of voltage (at negative polarity)

machining time causing the MRR to decrease. At this region of lower MRR at 2–4 A, the relative tool wear ratio increases. Moreover, with the increased discharge energy by increasing peak current, the crater size becomes broad and also the debris becomes too great in the gap which becomes difficult to remove from the machined area by side flushing. Therefore, arcing causes due to establishment of a conductive electrical path between the electrodes. As a result, more material is removed from the electrode compared with workpiece resulting in more relative tool wear ratio.

The spark gap decreases first with increase of peak current from 1 to 4 A; after that, it starts to increase linearly. This shows that there will be an optimum value of spark gap for different machining conditions. For this combination of parameters, the optimum value of peak current to produce the smallest spark gap is 4 A. The taper angle reduces first with the increase of peak current, remains steady up to 4 A, and then again tends to increase. The taper angle increases more at higher peak current as the electrode is worn laterally at higher discharge energy settings. The lateral wear causes tip of the electrode to decrease in diameter causing the taper. The reason for common taper in micro-EDM drilling is that the debris produced during machining moves from the bottom of hole and eject out from the top of hole along the outside of the electrode [18]. This phenomenon will create secondary sparks between the debris and the work piece, slightly enlarging the hole at the top, thus making the micro-hole taper [18, 19]. The circularity gets better as the current nears 3 A and the machined hole gets less round as the current increases further. This could be because when the

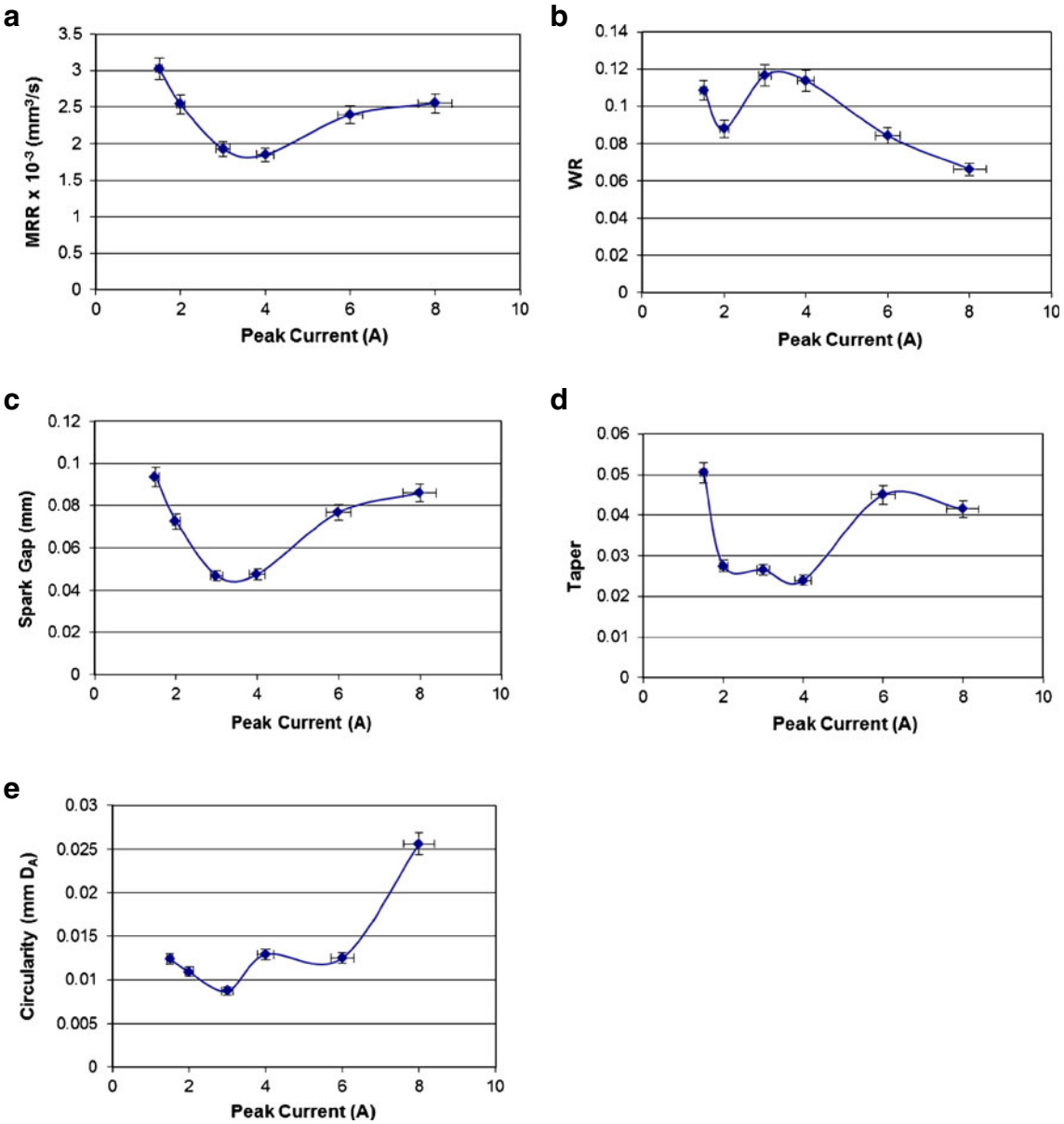

Fig. 6 Effect of peak current on **a** MRR, **b** WR, **c** spark gap, **d** taper, and **e** circularity of the micro-holes

current is too small, the sparks are ineffective resulting in irregular machining. When the current gets too large, the material removed per spark gets larger and the crater created is also larger resulting in bad finishing. High current generally produces greater surface roughness as the material removal rate is higher. Due to high machining rate, the amount of debris in the gap becomes high which results electrically conducting path between workpiece and electrode. This electrically conducting path finally causes arcing, which increases surface roughness in the workpiece. Figure 7 shows the comparison of performance parameters for the highest and the lowest setting of peak current. It can be seen that the micro-holes become much bigger in dimension at higher setting of peak current. In addition, the taper of the micro-hole also increases, which indicates that very high value of peak current is not suitable in terms of micro-structure accuracy and surface quality.

3.3 Effect of pulse duration

The effect of pulse duration (T_{on}) on different performance parameters are shown in Fig. 8. All other parameters are set at constant values of voltage of 200 V, peak current of 3 A, pulse interval of 50 μs, servo of 65%, and electrode rotational speed of 1,200 rpm.

The MRR increases with the increase of pulse duration at a decreasing rate, peaks when pulse duration is 25 μs, and decreases as the duration increases. This is

a

Fixed Parameters	Voltage	Pulse Duration	Pulse Interval	Servo	Tool Diameter	Rotation
	200 V	25 µs	50 µs	65	200µm	1200 rpm

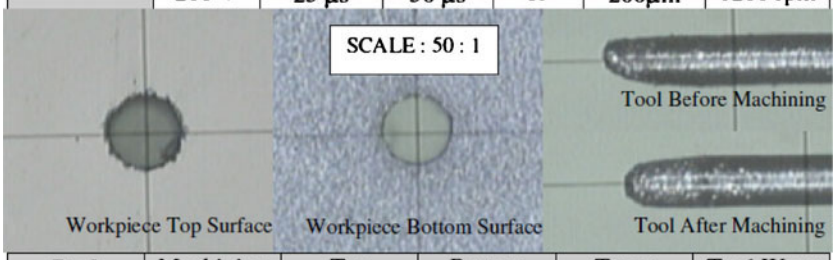

Peak Current	Machining Time	Top Diameter	Bottom Diameter	Taper	Tool Wear
3 A	16 s	293.5 µm	267.0 µm	0.0265	114.5 µm

MRR x 10^{-3}	WR	Spark Gap	Circularity
1.9270 mm^3/s	0.1166	0.0467 mm	0.0087

b

Fixed Parameters	Voltage	Pulse Duration	Pulse Interval	Servo	Tool Diameter	Rotation
	200 V	25 µs	50 µs	65	200µm	1200 rpm

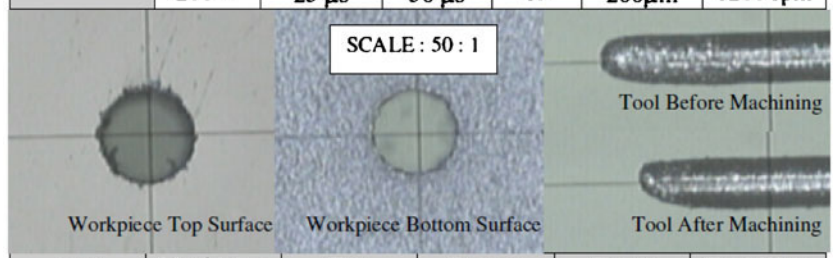

Peak Current	Machining Time	Top Diameter	Bottom Diameter	Taper	Tool Wear
8 A	19 s	372.0 µm	330.5 µm	0.0415	102.5 µm

MRR x 10^{-3}	WR	Spark Gap	Circularity
2.550 mm^3/s	0.0664	0.0860 mm	0.0256

Fig. 7 Comparison of performance parameters at the lowest and highest setting of peak current using positive polarity

because when pulse duration is too short, very little material is melted in each cycle, which results in lower MRR. At moderately higher pulse duration, the MRR increases as the duration of current for machining becomes higher. However, although very long pulse duration can melt more materials, these materials will only re-solidify and machining time will increase. Due to longer machining time, the MRR calculation shows decreasing trends at higher values of pulse duration. The electrode WR increases with the increase of pulse duration and remains steady with further increase of pulse duration. The WR rises sharply from 3.2 to 12.8 µs where it starts to decrease and remains steady for further increase of pulse duration. At 25 µs, the WR stays almost constant at about 0.08 and decreases slowly thereafter. The effect on MRR, spark gap, and taper is showing generally the same trend. The spark gap and taper peak at 12.8 µs pulse duration and remain unchanged or decreased after that. This shows that lateral tool wear is the highest when pulse duration is 12.8 µs. In case of circularity, it has been found that the micro-hole circularity becomes poor at very small value of pulse duration. However, at moderately higher pulse duration, the circularity improves and remains steady for long range of pulse duration. The machined micro-hole profile gets better near to pulse duration of 50 µs and gets less round as the duration increases further. When the pulse duration is too small, there is not enough time to melt the material properly resulting in irregular machining. On the other hand, too large a value of pulse duration, however, will result in too much material being melted and, thus, unable to be removed properly. The comparison of all the performance parameters at the lowest and highest values of pulse duration is summarized in Fig. 9.

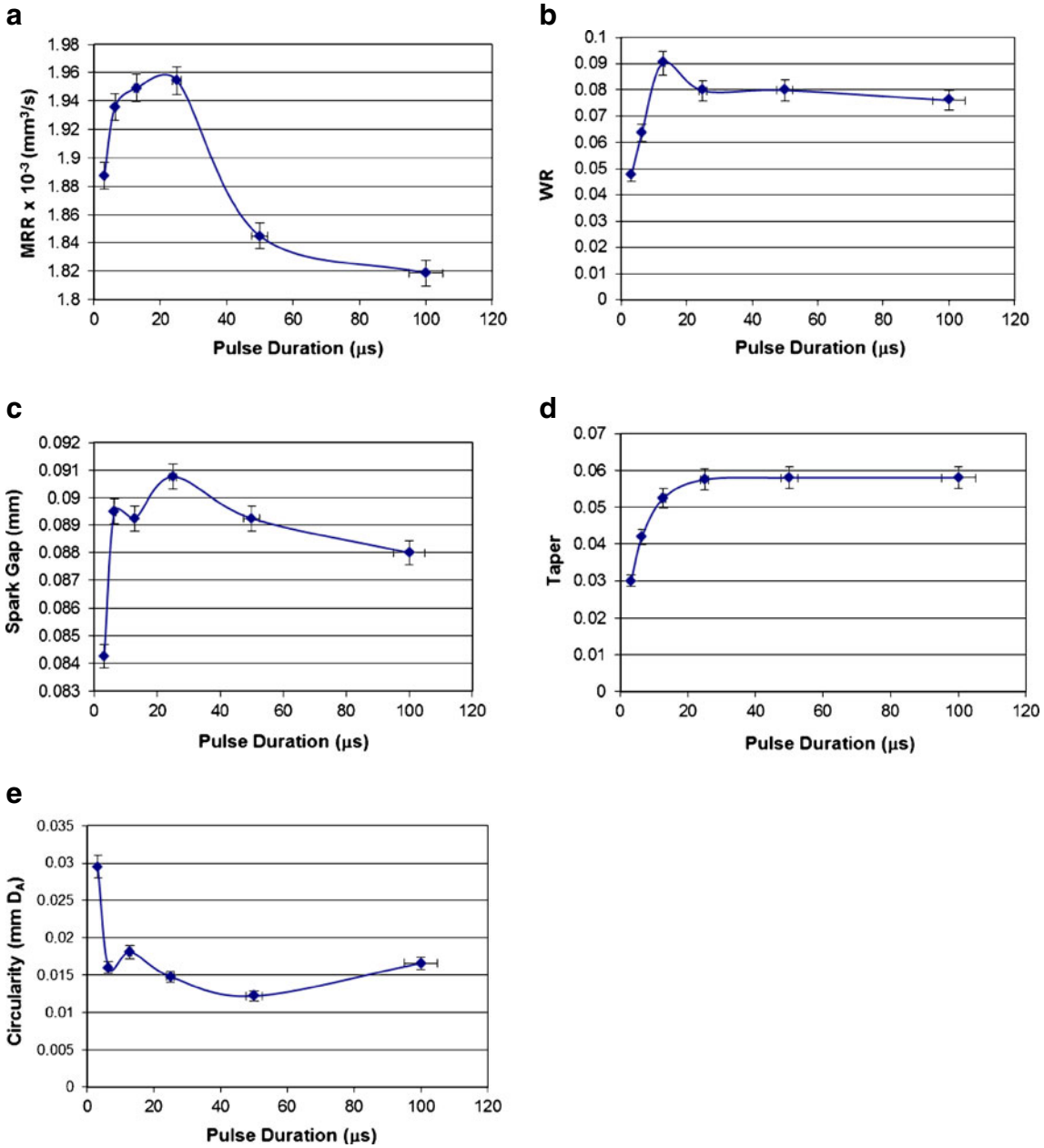

Fig. 8 Effect of pulse duration on **a** MRR, **b** WR, **c** spark gap, **d** taper, and **e** circularity of the micro-holes

3.4 Effect of pulse interval

The effect of pulse interval (T_{off}) on different performance parameters are shown in Fig. 10. All other parameters are set at constant values of voltage of 200 V, peak current of 3 A, pulse duration of 25 μs, servo of 65%, and electrode rotational speed of 1,200 rpm.

The MRR decreases almost linearly with the increase of pulse interval. However, it has been found that very small pulse interval does not favor the machining although more time is allowed for machining. This is due to the fact that continuous pulse duration does not allow enough time to remove the debris particles from the machined zone. Therefore, new materials cannot come in contact to sparking, resulting in reduction of MRR. In this study, the MRR peaks at medium value of pulse interval between 12.8 and 25 μs pulse interval. The pulse interval, which is the rest time, allows the melted materials to be removed by flushing. Therefore, it is about 20 μs that all melted materials can be removed. The WR is generally increasing as pulse interval increases. Therefore, using too large a value for pulse interval not only lengthens machining time but also increases tool wear. In case of spark gap, the values decrease with the increase of pulse interval. In case of taper angle, the results show inconsistent trend. The taper angles of micro-holes increase first with the increase of pulse

Fig. 9 Comparison of performance parameters at the lowest and highest setting of pulse duration using positive polarity

a

Fixed Parameters	Voltage	Peak Current	Pulse Interval	Servo	Tool Diameter	Rotation
	200 V	3 A	50 µs	65	200µm	1200 rpm

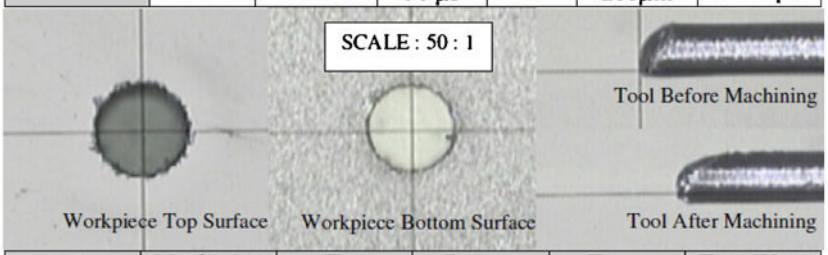

Pulse Duration	Machining Time	Top Diameter	Bottom Diameter	Taper	Tool Wear
3.2 µs	26 s	368.5 µm	338.5 µm	0.0300	74.5 µm

MRR x 10^{-3}	WR	Spark Gap	Circularity
1.8870 mm^3/s	0.0476	0.0842 mm	0.0295

b

Fixed Parameters	Voltage	Peak Current	Pulse Interval	Servo	Tool Diameter	Rotation
	200 V	3 A	50 µs	65	200µm	1200 rpm

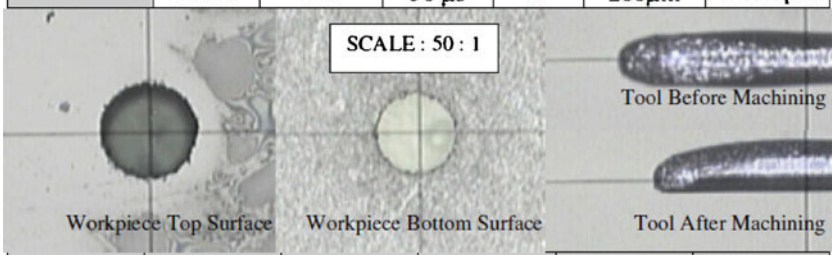

Pulse Duration	Machining Time	Top Diameter	Bottom Diameter	Taper	Tool Wear
100 µs	26 s	376.0 µm	318.0 µm	0.0580	114.4 µm

MRR x 10^{-3}	WR	Spark Gap	Circularity
1.8186 mm^3/s	0.0760	0.0880 mm	0.0166

interval and then decrease again at higher values of pulse intervals. The circularity improves as pulse interval increases. This is very obvious, as with the increase of pulse interval, more time is allowed to flush the debris particles from the machined zone, thus reducing the chance of secondary sparking. Therefore, the roughness at the profiles of micro-holes improves. Thus, rounder machined holes are produced with improved circularity. Figure 11 shows a summary of the different performance parameters calculated and images of micro-holes and tool electrodes at the lowest and highest setting of pulse interval.

3.5 Effect of servo

The effect of servo control parameter on different performance parameters is shown in Fig. 12. All other parameters are set at constant values of voltage of 200 V, peak current of 3 A, pulse duration of 25 µs, pulse interval of 50 µs, and electrode rotational speed of 1,200 rpm.

The servo controls the advance of the electrode on the workpiece. The value of the servo is expressed in percentage with 100% being the weakest and 0% being the strongest. Therefore, servo 65 compares the rates of electrode advances to the workpiece with other setting of servo percentage. Actually, it is an indication of movement speed of electrode toward workpiece during micro-EDM. It has been observed from Fig. 12 that the effects of servo on MRR, spark gap, taper, and circularity have almost similar trends. The values for these performance parameters decrease first as the servo value increases, a minimum is reached when servo value is 65, and the parameters increase after that. This shows that the servo value of 65 is optimum as it gives the best machined micro-hole profile and dimensional accuracy as indicated by the lower values for spark gap, taper, and circularity.

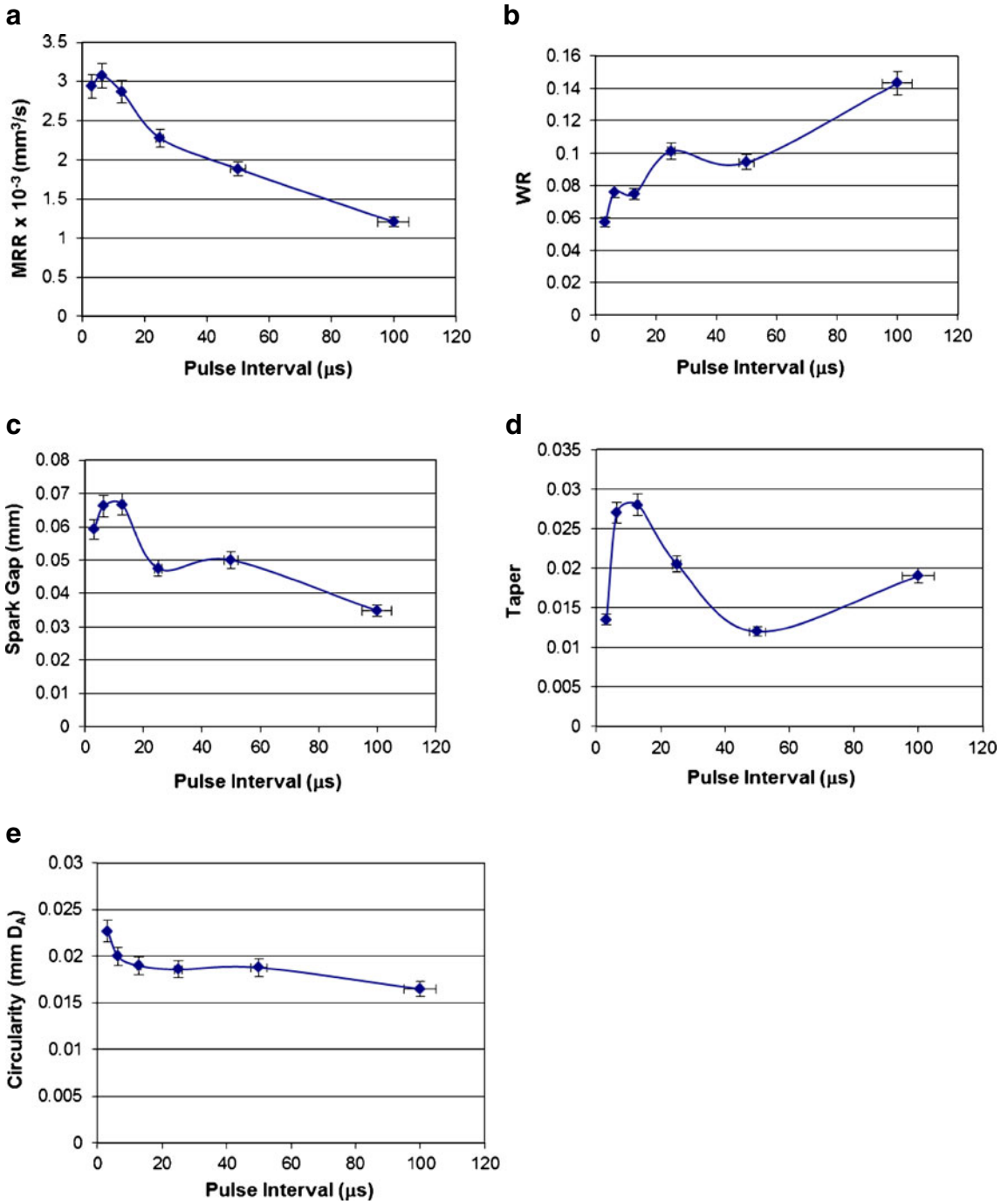

Fig. 10 Effect of pulse interval on **a** MRR, **b** WR, **c** spark gap, **d** taper, and **e** circularity of the micro-holes

However, at this value, MRR is also lower. If finished micro-hole profile is not of importance, other values of servo may be used. It is also noted that using small values of servo will increase the MRR, but the rough machining process might break the silicon workpiece, which is very difficult to machine. For the WR, there is no obvious trend in the curve; therefore, it is concluded that the WR is not affected greatly by the servo value. A summary of the different performance parameters and optical image of the workpiece and electrode at the lowest and highest setting of servo is presented in Fig. 13.

3.6 Effect of electrode rotation

The effect of electrode rotational speed on different performance parameters are shown in Fig. 14. All other

a

Fixed Parameters	Voltage	Peak Current	Pulse Duration	Servo	Tool Diameter	Rotation
	200 V	4 A	25 μs	65	200μm	1200 rpm

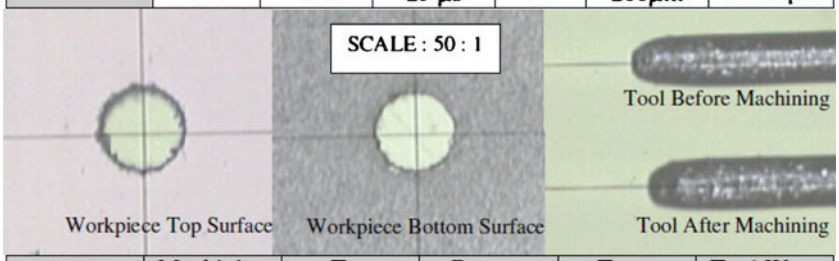

Pulse Interval	Machining Time	Top Diameter	Bottom Diameter	Taper	Tool Wear
3.2 μs	13 s	318.5 μm	305.0 μm	0.0135	69.5 μm

MRR x 10^{-3}	WR	Spark Gap	Circularity
2.9358 mm^3/s	0.0572	0.0592 mm	0.0227

b

Fixed Parameters	Voltage	Peak Current	Pulse Duration	Servo	Tool Diameter	Rotation
	200 V	4 A	25 μs	65	200μm	1200 rpm

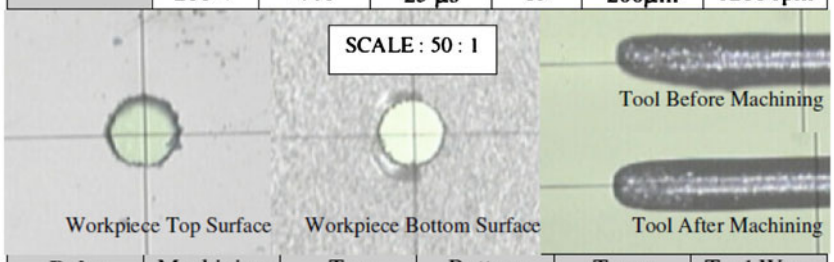

Pulse Interval	Machining Time	Top Diameter	Bottom Diameter	Taper	Tool Wear
100 μs	22 s	269.5 μm	250.5 μm	0.0190	121.0 μm

MRR x 10^{-3}	WR	Spark Gap	Circularity
1.2066 mm^3/s	0.1431	0.0347 mm	0.0165

Fig. 11 Comparison of performance parameters at the lowest and highest setting of pulse interval

parameters are set at constant values of voltage of 200 V, peak current of 3 A, pulse duration of 25 μs, pulse interval of 50 μs, and servo of 65%.

The trend in the curves for MRR, spark gap, and taper is very similar. As no flushing is used, the rotation aids in the removal of melted material. Higher rotation facilitates the removal of melted material, but beyond the optimum value, the actual machining process may be affected as the electrode is moving too fast. The increase in MRR is due to the fact that with increase of electrode rotational speed, the tangential velocities of the electrode increase which promote the disturbance of the dielectric [20, 21]. The increased flow speed of the dielectric helps to depart the debris from the machined zone, thus facilitating further material removal from the workpiece. The WR decreases sharply with the increase of electrode rotational speed. The reason behind this can also be explained by the effect of tangential velocity of the electrode. As the tangential velocity of electrode is low at lower speed, the debris cannot be removed from the machined zone easily. Thus, continuous sparking occurs at these debris which causes arcing. During this arcing, more material is removed from the electrode instead of removing new materials from the workpiece. In case of spark gap, first it increases slightly with the increase of electrode rotational speed up to 500 rpm, and then again the value of spark gap decreases steadily. This is because increasing the electrode rotational speed can improve the discharge of debris that reduces the spark gap. A lower value of spark gap is an indicative of better dimensional accuracy.

The value of 1,200 rpm gives the lowest tool wear ratio, lower spark gap, taper, and circularity, thus

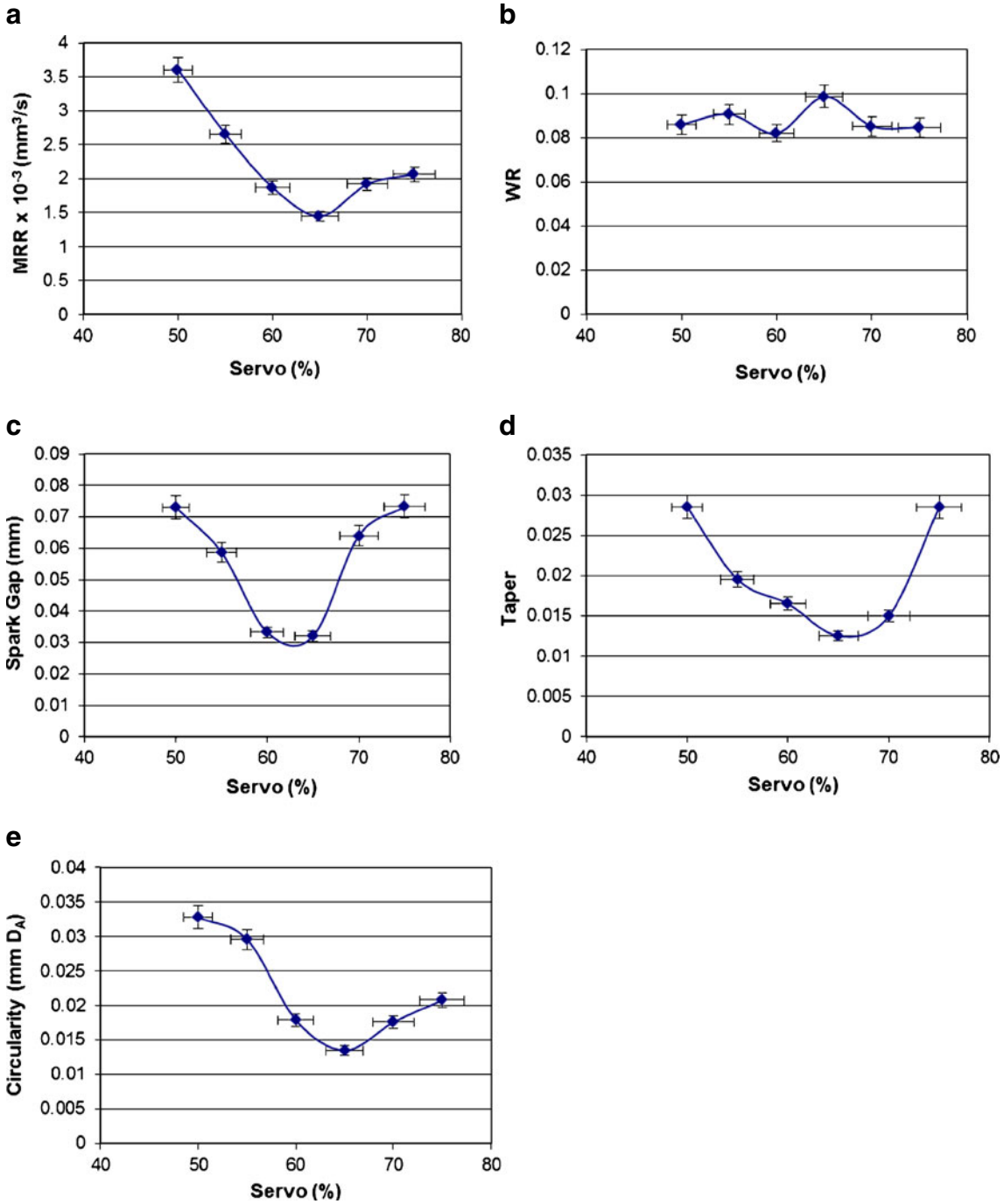

Fig. 12 Effect of servo on **a** MRR, **b** WR, **c** spark gap, **d** taper, and **e** circularity of the micro-holes

considered as optimum setting. When no rotation is used, the WR is as high as 0.1083 and the hole is not very round as shown by the large value of actual deviation in circularity; however, it shows very little taper and small spark gap (Fig. 15). This is due to the fact that the electrode might be slightly misaligned during machining. Rotating the electrode will thus provide a rounder and larger hole.

4 Micro-structuring in silicon

4.1 Micro-hole machining using microelectrodes fabricated on-machine by block-μEDM

As the electrode diameters get smaller, any minor misalignments may have a significant effect on the final output values obtained. Therefore, an on-machine process is

Fig. 13 Comparison of performance parameters at the lowest and highest setting of servo

a

Fixed Parameters	Voltage	Peak Current	Pulse Duration	Pulse Interval	Tool Diameter	Rotation
	200 V	6 A	25 µs	50 µs	200µm	1200 rpm

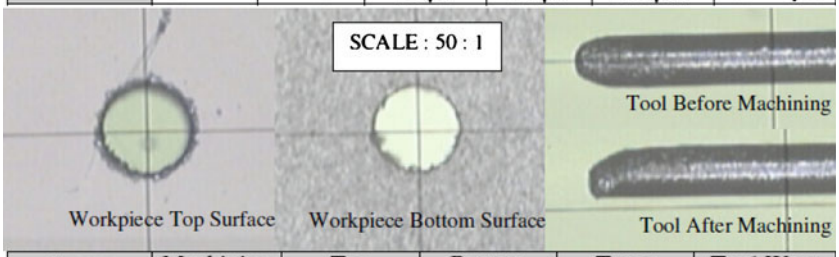

Servo	Machining Time	Top Diameter	Bottom Diameter	Taper	Tool Wear
50	12 s	346.0 µm	317.5 µm	0.0285	118.5 µm

MRR x 10^{-3}	WR	Spark Gap	Circularity
3.6016 mm^3/s	0.0861	0.0730 mm	0.0328

b

Fixed Parameters	Voltage	Peak Current	Pulse Duration	Pulse Interval	Tool Diameter	Rotation
	200 V	6 A	25 µs	50 µs	200µm	1200 rpm

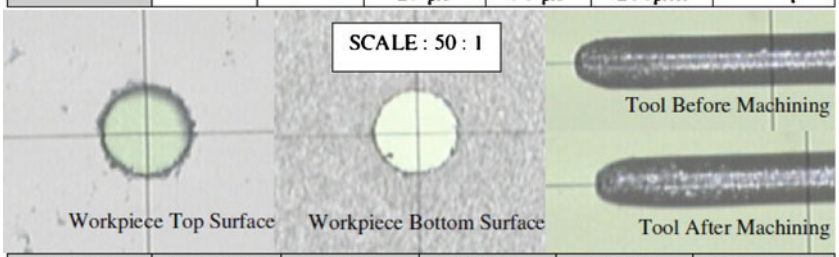

Servo	Machining Time	Top Diameter	Bottom Diameter	Taper	Tool Wear
75	21 s	346.5 µm	318.0 µm	0.0285	117.0 µm

MRR x 10^{-3}	WR	Spark Gap	Circularity
2.0642 mm^3/s	0.0847	0.0732 mm	0.0208

designed to machine the electrode to the required dimension and then using this electrode to machine a vertical through hole in the silicon workpiece.

The microelectrode is produced from a 0.5-mm electrode which is machined laterally until the desired dimension is obtained. The process starts by edging being done on the *Z*-axis and then on the *X*-axis. Figure 16 shows the schematic diagram of the block-µEDM process [22]. It needs a precise sacrificial rectangular block with high wear resistance (WC was used in this study due to its high resistance to wear) and a commercially available electrode. However, one important thing is the alignment of block respective to the electrode. It is very important that sacrificial block should be aligned properly (within an accuracy of ±2 µm) in order to avoid electrodes being more taper, thus reducing dimensional accuracy [22]. It has been found that due to wear of the sacrificial block also, the diameter of the fabricated electrode is sometimes difficult to predict. In this method, the block is used as a cutting electrode, and a cylindrical rod is used as the workpiece in the EDM process. The microelectrode that needs to be machined is fed against the conductive block. The machining is carried out by applying a controlled electric spark and by forcing the dielectric medium to flow through the spark gap between the block and the rod. A small amount of the material is eroded from both the block and the rod and is carried away by the flushing medium.

Figure 17 shows the dimensions of the target microelectrode, and Table 3 shows the input parameters used for machining the microelectrode. The values presented in Fig. 17 are estimated using the experience gained from earlier parts of the experiment and tested using trial and error. After the electrode has been made, it is brought to as close to the workpiece surface as possible, and reference is

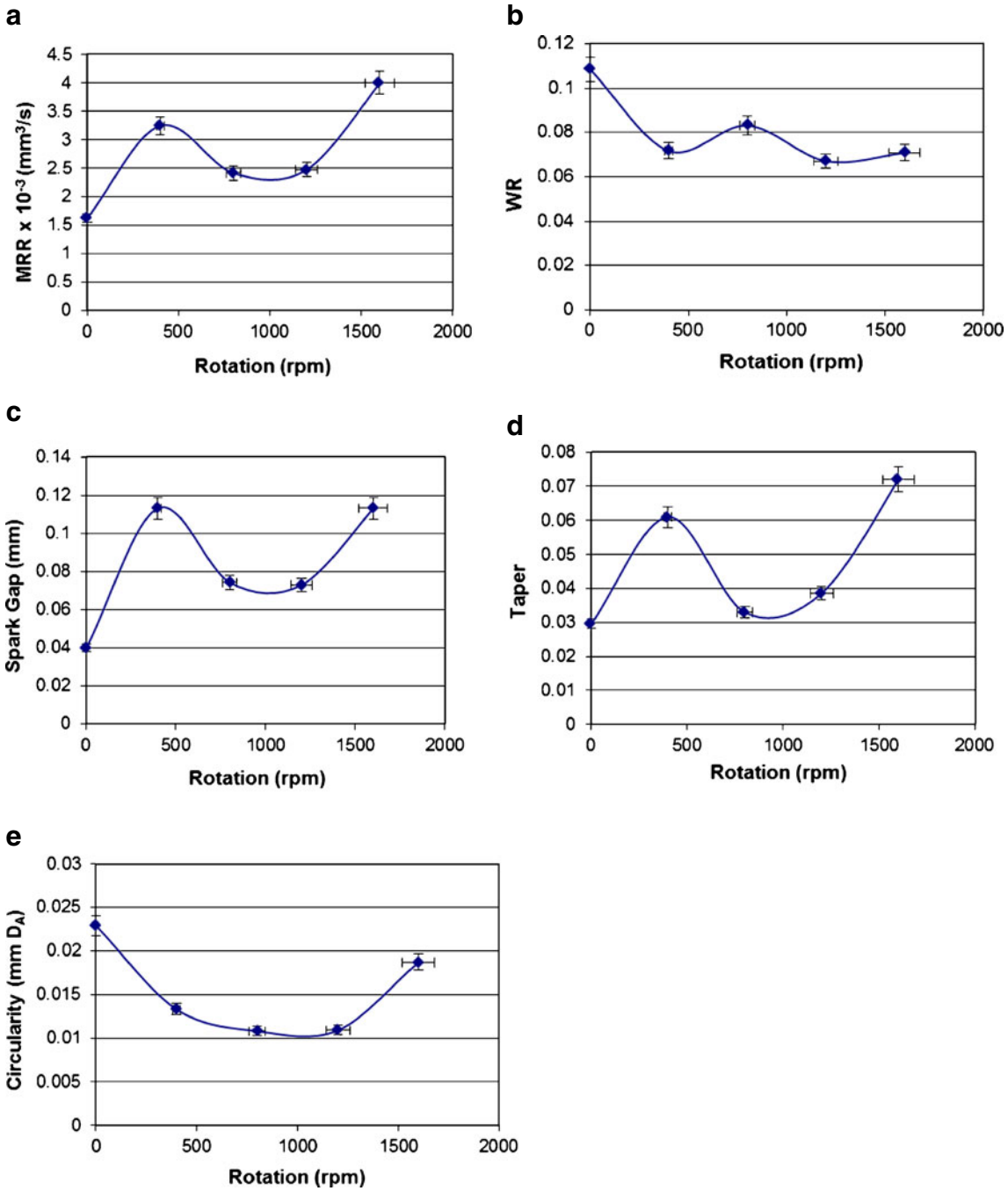

Fig. 14 Effect of electrode rotational speed on **a** MRR, **b** WR, **c** spark gap, **d** taper, and **e** circularity of the micro-holes

made when the electrode just touches the layer of dielectric left on the workpiece after the work tank is drained. This is done as edging using the machine tends to bend these microelectrodes. After this "manual edging process," the machining is done. The only exception is that the electrode length could not be measured before machining, as there is no on-machine measuring system and bringing the electrode to the video measuring system will induce misalignment when it is replaced.

For this part of the experiment, the smallest electrode diameter achievable is 40 μm, and the smallest hole is 70 μm in diameter (see Fig. 18). From the results, micro-hole diameter is about double the electrode diameter for all cases. For smaller voltages, the spark gap tends to be smaller. The profile for the machined holes gets better as current decreases. The hole with the best circularity is produced with a 0.0495-mm electrode and using a peak current of 1.5 A (see Fig. 19). Using electrodes of diameter

a

Fixed Parameters	Voltage	Peak Current	Pulse Duration	Pulse Interval	Servo	Tool Diameter
	200 V	4 A	25 µs	50 µs	65	200 µm

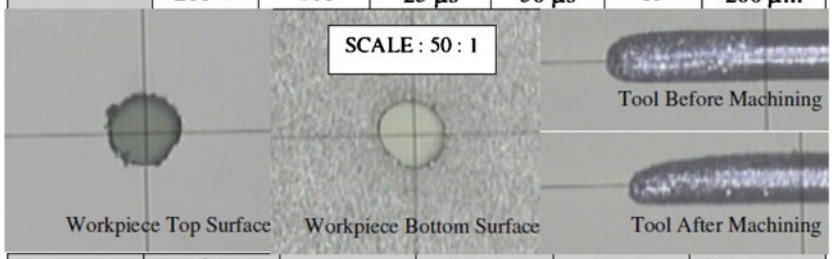

Rotation	Machining Time	Top Diameter	Bottom Diameter	Taper	Tool Wear
0 rpm	17 s	279.6 µm	250.0 µm	0.0296	95.0 µm

MRR x 10^{-3}	WR	Spark Gap	Circularity
1.6197 mm^3/s	0.1083	0.0398 mm	0.0229

b

Fixed Parameters	Voltage	Peak Current	Pulse Duration	Pulse Interval	Servo	Tool Diameter
	200 V	4 A	25 µs	50 µs	65	200 µm

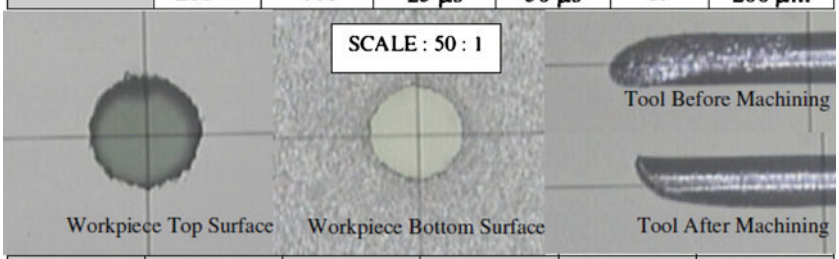

Rotation	Machining Time	Top Diameter	Bottom Diameter	Taper	Tool Wear
1600 rpm	15 s	426.5 µm	354.5 µm	0.0720	135.0 µm

MRR x 10^{-3}	WR	Spark Gap	Circularity
3.9920 mm^3/s	0.0708	0.1132 mm	0.0187

Fig. 15 Comparison of performance parameters at the lowest and highest setting of electrode rotational speed

of about 50 µm, smaller voltages will give small spark gaps. Therefore, for better control of the machined micro-hole dimensions, small voltages should be used as they provide smaller spark gaps.

4.2 Machining of micro-slots

Four slots are machined in this part of the experiment using the same parameters. The different ways used to machine the slots will make the profile of the slots slightly different. Table 4 shows the parameters used for machining the slots. The image of the slots and the tools before and after machining are presented in the same figure as seen in Figs. 20 and 21.

The four methods used for micro-slot machining in silicon workpiece are:

1. Using a single pass from left to right
2. Using three passes in the same direction (left to right)
3. Using six passes in alternating directions
4. Using a single pass from left to right (through slot)

The slots are machined to a depth of 0.3 mm for the blind slots, while the through slot is machined to a depth of 0.8 mm.

From the results, the slot machined by six passes gives the best profile as the slot is more even and there is better surface finish (see Fig. 20c). The finish of the slot produced by using three passes in the same direction is also quite good (see Fig. 20b); however, it is slightly bigger at the starting end than the ending end. The slot produced using a single pass has bad surface finish, and also the difference in size on both ends is very significant (see Fig. 20a).

The through hole also has large differences in dimension at both ends, as the slot is machined by a single pass. The main reason for the difference in dimension at the entrance

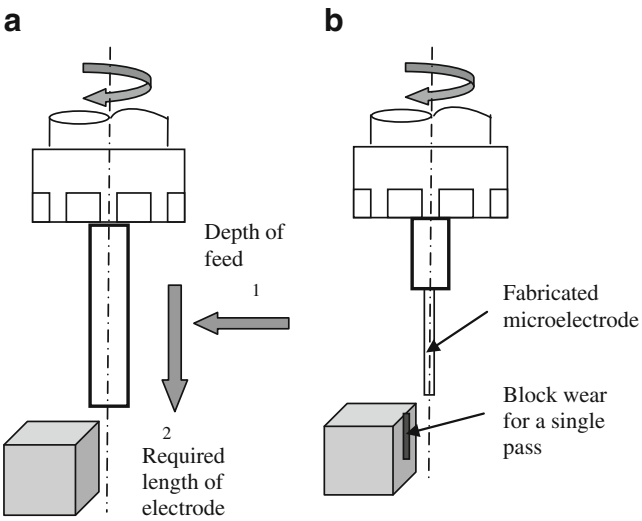

Fig. 16 Schematic diagram representing the block-μEDM process: **a** at the beginning of process; **b** fabricated microelectrode

and exit is the electrode wear, as the diameter reduces as machining continues from left to right. Also at the cross section at the ending end is "C"-shaped, as the tool wear is very uneven (see Fig. 21). The electrode being slightly misaligned may also cause this effect, as only one side of the electrode is used to machine. A better method to machine through slots would be to use multiple passes and machining from both sides one after another and progressively machine deeper into the workpiece. The only disadvantage is that machining may take longer time.

5 Conclusions

In this study, the feasibility of machining p-type silicon by electrodischarge machining was investigated. The effect of major operating parameters on the EDM performance of silicon has been presented. Microelectrodes are fabricated successfully on the conventional EDM machine for machining micro-holes and micro-slots in silicon. From the detail experimental investigations, the following conclusions can be drawn:

- With the increase of gap voltage, the value of MRR, WR, and spark gap increases but surface becomes rougher, which results in higher values of circularity. For both positive and negative voltage, the trends are the same but reverse in shape, which means p-type silicon is machinable by EDM using both the polarities.
- With the increase of peak current, the MRR, spark gap, taper, and circularity decrease first then again tend to increase at higher values of peak current. Very lower value of peak current is not favorable for improved performance as well as micro-hole dimensional accuracy.
- With the increase of pulse duration, the MRR, WR, taper, and spark gap increase. However, excessive pulse

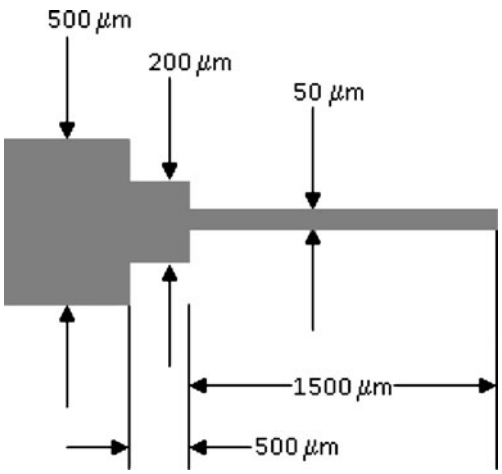

Fig. 17 Final target dimension of the microelectrode

Table 3 Parameters for the fabrication of the microelectrodes

Process	Rough cut	Finishing
Voltage, V	200	200
Peak current, A	3	1.5
Pulse duration, μs	25	3.2
Pulse interval, μs	50	50
Servo	65	65
Rotation, rpm	1,200	1,200
Method of flushing	Jet (side) flushing	Jet (side) flushing

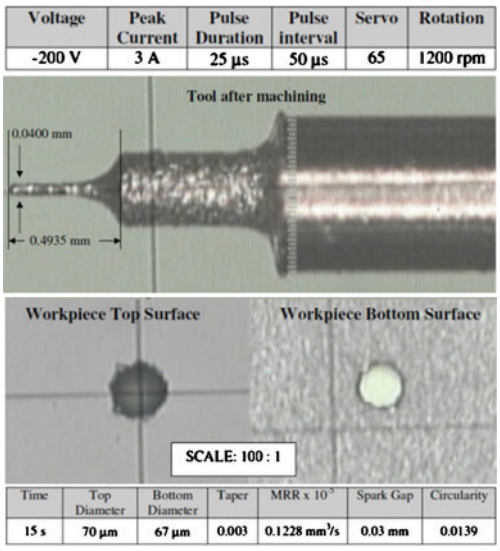

Fig. 18 Fabrication of 40 μm electrode with 500 μm length (a.r. 12) using block-μEDM process and fabricated micro-holes in silicon workpiece

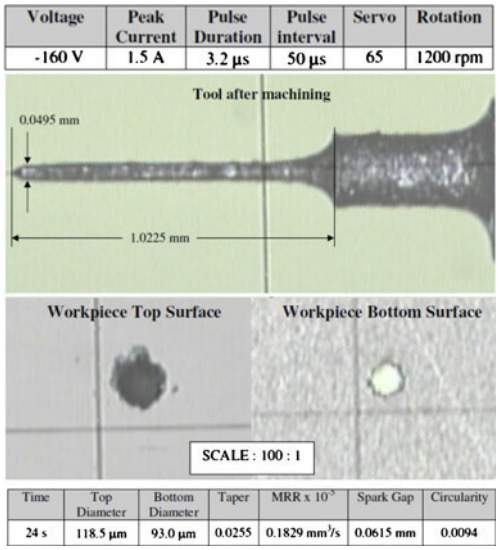

Fig. 19 Fabrication of 50 µm electrode with 1,000 µm length (a.r. 20) using block-µEDM process and fabricated micro-holes in silicon workpiece

duration can be counter-productive in case of MRR. Very low pulse duration not only provides lower MRR but also provides poor micro-hole profiles in terms of roundness and circularity. Selection of optimum pulse duration is thus important.

- The MRR, spark gap, taper, and circularity decrease steadily with the increase of pulse off-time. The relative electrode WR increases gradually with the increase of pulse interval. However, very lower value of pulse interval is not favorable for maintaining machining stability.
- The values for all the performance parameters decrease as the servo value increases, a minimum is reached at optimum servo value, and the parameters increase after that. Only the WR was found to be unaffected by the servo.
- The MRR increases and WR decreases with the increase of electrode rotational speed. Electrode rotation can significantly enhance the overall performance of the micro-EDM as well as improve dimensional accuracy and surface finish of the micro-holes.

Table 4 Parameters used for machining slots

Voltage, V	200
Peak current, A	3
Pulse duration, µs	25
Pulse interval, µs	50
Servo	65
Rotation, rpm	1,200
Flushing	No flushing

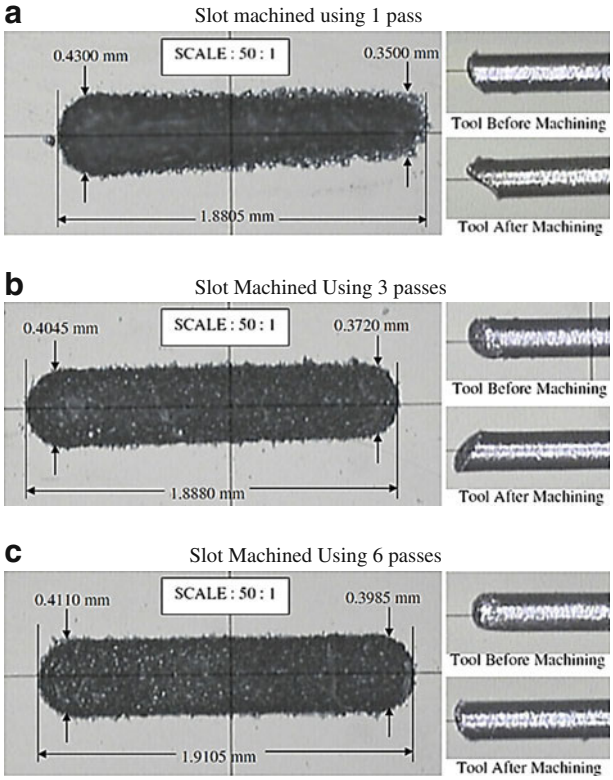

Fig. 20 A photograph showing the machined blind slots by different passes

- From the experiments, the machining conditions that are found favorable for improved micro-EDM of p-type silicon are as follows:
  (a) Voltage from 160 to 200 V
  (b) Peak current of about 3 to 4 A
  (c) Pulse duration of 25 µs
  (d) Pulse interval of 50 µs
  (e) Servo of 65%
- The machining of smaller diameter and higher aspect ratio micro-holes is carried out with on-machine

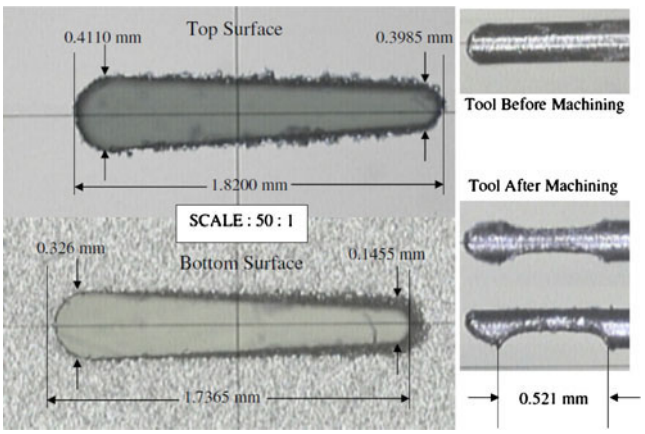

Fig. 21 Optical image of the machined through slot using 1 pass

fabricated microelectrodes as small 40 μm. The micro-slots can be fabricated with improved surface finish and better dimensional accuracy by using lower gap voltage, peak current, and using multiple numbers of passes. To conclude, the possibilities of performing micromachining of silicon on a conventional EDM machine have been proven successful.

6 Recommendations for future research

Although the experiments are carried out successfully, some of the results can be improved further. An on-machine optical measuring system would be very useful in aligning the electrode to the machine axis and to measure the electrode length and diameter before and after machining without removing it from the rotary unit. Modifications can also be made to the work tank to allow machining in deionized water using other electrode materials like copper tungsten, silver tungsten, etc. The study could also be done using the micro-EDM machine, as the machine is made for the purpose of micromachining and may produce better results than the conventional machine. Moreover, the lowest settings of gap voltage, peak current, will be much lower in micro-EDM machine, which will enable further reduction of discharge energy, thus more miniaturization of products.

References

1. Reynaerts D, Heeren PH, Brussel HV (1997) Microstructuring of silicon by electro-discharge machining (EDM)—part I: theory. Sens Actuators A 60:212–218
2. Masaki T, Kawata K, Masuzawa T (1990) Micro electro discharge machining and its applications. In: Proc IEEE. Napa valley, CA, USA, 11–14 Feb, pp 21–26
3. Luo YF, Chen CG, Tong ZF (1992) Investigation of silicon wafering by wire EDM cutting. J Mater Sci 27:5805–5810
4. Luo YF, Chen CG, Tong ZF (1992) Slicing thin silicon wafers by wire EDM cutting, In: Proc Int Symp Electromachining. Magdeburg, Germany, 6–8 May, pp 287–294
5. Langen HH, Masuzawa T, Fujino M (1995) Modular method for microparts machining and assembly with self-alignment. Ann CIRP 44:173–176
6. Staufert G, Dommann A, Läuger D (1993) Behaviour of a silicon spring fabricated by wire electro-discharge machining. J Micromech Microeng 3:232–235
7. Heeren PH, Reynaerts D, Brussel HV, Beuret C, Larsson O, Bertholds A (1997) Microstructuring of silicon by electro-discharge machining (EDM)—part II: applications. Sens Actuators A 61:379–386
8. Reynaerts D, Brussel HV (1999) Micro-EDM: a versatile technology for silicon micromachining. Int J Jpn Soc Precis Eng 33(2):114–119
9. Reynaerts D, Meeusen W, Brussel HV (1998) Machining of three-dimensional microstructures in silicon by electro-discharge machining. Sens Actuators A 67:159–165
10. Reynaerts D, Meeusen W, Brusel HV, Reynjens S, Puers R (1999) Production of seismic mass suspension in silicon by electro-discharge machining. J Micromech Microeng 9:206–210
11. Rakwal D, Heamawatanachai S, Tathireddy P, Solzbacher F, Bamberg E (2009) Fabrication of compliant high aspect ratio silicon microelectrode arrays using micro-wire electrical discharge machining. Microsyst Technol 15(5):789–797
12. Kunieda M, Ojima S (2000) Improvement of EDM efficiency of silicon single crystal through ohmic contact. Precis Eng 24:185–190
13. Takino H, Ichinohe T, Tanimoto K, Yamaguchi S, Nomura K, Kunieda M (2004) Cutting of polished single-crystal silicon by wire electrical discharge machining. Precis Eng 28(3):314–319
14. Weng FT, Hsu CS, Lin WF (2006) Fabrication of micro components to silicon wafer using EDM process. Mater Sci Forum 505–507:217–222
15. Song X, Reynaerts D, Meeusen W, Brussel HV (1999) Investigation of micro-EDM for silicon microstructure fabrication, design, test, and microfabrication of MEMS and MOEMS In: Proceeding of conference Paris, FRANCE (30/03/1999) 3680(2), pp 792–799
16. Charmilles Technologies (2010) Roboform 40 series machine manual. http://www.charmillesus.com/service/parts/catalog/machines/FO40/index.htm. Last accessed 3 Sep 2010
17. Ross RB (1992) Metallic materials specification handbook, 4th edn. Chapman and Hall, London, p 284, 606
18. Jahan MP, Wong YS, Rahman M (2010) A comparative experimental investigation of deep-hole micro-EDM drilling capability for cemented carbide (WC-Co) against austenitic stainless steel (SUS 304). Int J Adv Manuf Technol 46(9–12):1145–1160
19. Takahata K, Aoki S, Sato T (1996) Fine surface finishing method for 3-dimensional micro structures. In: Proceedings of micro electro mechanical systems, 1996, MEMS '96, 11–15 Feb 1996, pp 73–78
20. Jahan MP, Wong YS, Rahman M (2009) A study on the quality micro-hole machining of tungsten carbide by micro-EDM process using transistor and RC-type pulse generator. J Mater Process Technol 209(4):1706–1716
21. Yan BH, Huang FY, Chow HM, Tsai JY (1999) Micro-hole machining of carbide by electrical discharge machining. J Mater Process Technol 87:139–145
22. Jahan MP, Rahman M, Wong YS, Fuhua L (2010) On-machine fabrication of high-aspect-ratio microelectrodes and application in vibration-assisted micro-EDM drilling of tungsten carbide. Proc Inst Mech Eng B J Eng Manuf 224(5):795–814